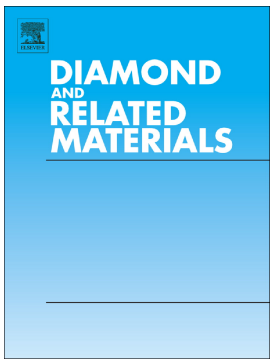

Conversion of paper and xylan into laser-induced graphene for environmentally friendly sensors

Bohdan Kulyk, Marina Matos, Beatriz F.R. Silva, Alexandre F. Carvalho, António J.S. Fernandes, Dmitry V. Evtuguin, Elvira Fortunato, Florinda M. Costa

PII: S0925-9635(22)00037-1

DOI: https://doi.org/10.1016/j.diamond.2022.108855

Reference: DIAMAT 108855

To appear in: *Diamond & Related Materials*

Received date: 6 November 2021

Revised date: 28 December 2021

Accepted date: 16 January 2022

Please cite this article as: B. Kulyk, M. Matos, B.F.R. Silva, et al., Conversion of paper and xylan into laser-induced graphene for environmentally friendly sensors, *Diamond & Related Materials* (2021), https://doi.org/10.1016/j.diamond.2022.108855

Conversion of paper and xylan into laser-induced graphene for environmentally friendly sensors

Bohdan Kulyk[a,b], Marina Matos[c], Beatriz F. R. Silva[a,d], Alexandre F. Carvalho[a,d], António J. S. Fernandes[a,]*, Dmitry V. Evtuguin[c], Elvira Fortunato[b], Florinda M. Costa[a,]*

[a]i3N – Institute for Nanostructures, Nanomodelling and Nanofabrication, Department of Physics, University of Aveiro, Aveiro 3810-193, Portugal

[b]i3N/CENIMAT, Department of Materials Science and CEMOP/UNINOVA, NOVA School of Science and Technology, NOVA University Lisbon, Campus de Caparica, 2829-516 Caparica, Portugal

[c]CICECO – Aveiro Institute of Materials, Department of Chemistry, University of Aveiro, Aveiro 3810-193, Portugal

[d]CICECO – Aveiro Institute of Materials, Department of Physics, University of Aveiro, Aveiro 3810-193, Portugal

*Corresponding authors: toze2@ua.pt, fiem@ua.pt

Abstract

Laser-induced graphene (LIG) is a foam-like porous material consisting of few-layer graphene obtained by laser irradiation of a wide range of carbon-containing substrates. Among these, the ability to synthesize LIG from paper and other cellulose-related materials is particularly exciting, as it opens the door to a wide assortment of potential applications in the form of low-cost, flexible, and biodegradable devices. Here, the synthesis of this material, dubbed paper-LIG, on different types of filter papers and xylan biopolymer is discussed. In particular, we report the formation of paper-LIG by single-step irradiation, providing an improvement over the conventional multiple lasing approach and giving an explanation of the conditions that allow this simplified synthesis. All the relevant process parameters are covered, assessing their effect on the resulting electrical properties, structure, and morphology. Additionally, we demonstrate the application of LIG obtained from xylan, an abundant and often underutilized biopolymer, for temperature sensing. These results provide a better understanding of the conditions required for the synthesis of highly conductive LIG from paper and related

materials, paving the way for its application, with reduced cost and low environmental impact, in fields ranging from biomonitoring to consumer electronics.

Keywords

Graphene, LIG, paper, xylan, sensors, laser, biopolymers

1. Introduction

The emergence of graphene in 2004 as a novel material with outstanding properties[1] has captivated the attention of not just the scientific community, but of the world at large. Motivated by the promise of scientific discovery and groundbreaking applications, this interest spurred an ever-growing body of work.[2] Remarkably, the world of graphene turned out to be even richer than perhaps initially expected, with a wide range of different types of graphene-based materials. From chemical vapor deposited large area single-layer graphene films with extremely high charge carrier mobilities[3] and large crystal sizes,[4] to the easily processable liquid-phase exfoliated few-layer graphene flakes,[5,6] each class of graphene-based materials shows unique properties which make them ideally suited for their respective fields of application.

One of the most recent additions to the graphene family is laser-induced graphene (LIG).[7] The first report concerning its synthesis was given in 2014, by the group of James M. Tour, describing porous 3D-structures composed of few-layer graphene, obtained by CO_2 laser (10.4 µm) irradiation of flexible commercial polymers such as polyimide.[8] This ability to easily pattern conductive paths onto flexible substrates motivated great interest, spurred by the demonstration of applications in sensing,[9,10] actuation[11] and energy storage,[8] among others. Since then, the formation of LIG has been achieved using laser radiation with different wavelengths,[9,10] as well as using other materials as precursors, such as wood,[12] cork[10] and paper.[13,14] Among these, paper is a particularly attractive one, being extremely versatile, cheap, lightweight and biodegradable. After the initial report of the use of paper for the synthesis of laser-induced graphene in 2018, this material, also referred to as *paper-LIG*, has already shown potential in several different fields.[15–21] Still, having been recently discovered, there are many unanswered questions about the synthesis process of *paper-LIG*.

In this work, we attempt to shed light on some of these questions. Namely, we systematically explore the formation of *paper-LIG* from activated charcoal filter paper. Secondly, we report the synthesis of this material from common filter paper using a single irradiation step, not only improving on the conventional multiple lasing process, but also providing an explanation of the mechanisms and conditions which allow it. Lastly, we show, for the first time (to the best of our knowledge), the formation of laser-induced graphene from xylan, an abundant, environmentally friendly biopolymer, demonstrating its proof-of-concept application in temperature sensing. These results further the understanding of the laser-induced graphene formation process from paper and related materials, widening the array of precursor substrates and resulting materials, as well as encouraging their future applications.

2. Experimental

2.1. Laser-induced graphene synthesis from filter paper

Cellulose filter paper with activated charcoal by Prat Dumas (500 μm of thickness, 160 g m^{-2}) and hardened ashless cellulose filter paper by Cytiva (Whatman grade 40, 95 g m^{-2}, 210 μm of thickness, ≤0.007% ash content) were sprayed with a commercial phosphate-based fire retardant (Anti-Flame by BBT), prior to irradiation by a K40 CO_2 (10.6 μm) continuous wave 40 W laser engraver, by Liaocheng Julong CO. Ltd. The latter was operated in a unidirectional line scan mode. The parameters varied throughout this work were laser power, beam scan speed and distance (separation) between scan lines. The laser powers used throughout this work were 700 mW, 800 mW and 900 mW, corresponding to power densities of 45.5 W mm^{-2}, 51.9 W mm^{-2} and 58.4 W mm^{-2} in focus, and 4.8 W mm^{-2}, 5.5 W mm^{-2} and 6.2 W mm^{-2} at 9 mm below focus, respectively (nominal focal length of the lens is 50.8 mm). For the synthesis of LIG from activated charcoal filter paper, two irradiation steps were employed. In the first one the paper was placed 9 mm below focus, while in the second one it was irradiated in focus. For the study of *paper-LIG* formation with a single irradiation step, the filter paper was fixed at the focal plane. In all instances the irradiated area was 6×6 mm^2.

2.2. Xylan film preparation and laser-induced graphene synthesis

Xylan was isolated from *Eucalyptus globulus* bleached kraft pulp by extraction with 10% NaOH according to previously described procedure.[22] Carboxymethyl xylan synthesis was carried out according to the method developed by Petzold et al.[23] Xylan was dissolved in NaOH aqueous solution (5M), and vigorously stirred at 30 ºC for 30 min. After that, sodium chloroacetate (SCA) was added to the mixture and the temperature was raised up to 65 ºC for 60 min. Carboxymethyl xylan was then neutralised by the addition of sulfuric acid until pH ~7, and further dialysed in a tubing, benzoylated with molecular weight cut-off 2000 Da, to remove salts. Subsequently, the dialysed carboxymethyl xylan was freeze-dried. The synthesis procedure was performed with the molar ratio of 1:2:4 for xyl:SCA:NaOH.

Carboxymethyl xylan films were prepared by the solvent casting approach. Specifically, carboxymethyl xylan (1 g) was dissolved in distilled water (2%, 50 mL) under magnetic stirring for 3 h. The solution was then deposited into a square Teflon mould (7 cm^2) and the films were cast, at 45 ºC for 96 h at relative humidity of 50 %. For the synthesis of LIG, the obtained films were then sprayed with a commercial phosphate-based fire retardant (Anti-Flame by BBT), fixing the films onto filter paper to provide support. Two irradiation steps were employed, at 9 mm below focus and in focus, with 1 W of irradiation power, 30 mm s^{-1} of scan speed and a line separation of 0.1 mm.

2.3. Material characterization

Optical photographs of the samples were acquired with a UI-3880CP-C-HQ R2 CMOS 6.41 MP camera, by IDS, through a stereo microscope, using both front and back lighting. Secondary and backscattered electron scanning electron microscopy (SE-SEM and BSE-SEM) images were acquired using Vega 3 SBH system, by TESCAN, with an acceleration voltage of 15 kV and a working distance of 15 mm. Raman spectroscopy was performed using a Jobin Yvon HR800 Raman system, by Horiba, and a He-Cd 441.6 nm laser, with a ×50 lens (NA = 0.5), by Olympus. A neutral density filter OD = 1 was used to attenuate the laser power to prevent any potential thermally induced chemical modification of the samples. Sheet resistance measurements were performed by the van der Pauw method, using a Keysight B2902A dual-channel source meter unit.

2.4. Preparation and testing of the xylan film temperature sensor

A temperature sensor employing LIG obtained from modified xylan was prepared by irradiating a 6×12 mm^2 area of the xylan film fixed onto filter paper, using 1.5 W of

power, 30 mm s^{-1} as the scan speed and a line separation of 0.1 mm. Silver paste was used to connect tin-coated 20 awg copper wires at each end of the sensor. To test the response to temperature, the sensor was placed over a TECD2S Peltier element, controlled by a MTDEVAL1 board by ThorLabs. The temperature was varied in 5 °C steps over a 20 °C to 45 °C range, while the resistance of the LIG sensor (along the conductive path) was measured by a Keysight B2902A source meter unit, applying a constant voltage of 0.05 V. Each temperature value was held for ~90 s and the resistance values of the last 30 s of each stage were averaged to obtain the response of the sensor at that temperature. Additional real-time measurements were performed by repeatedly alternating the temperature between 30 °C and 35 °C, as well as by varying it in steps of 1 °C steps in the range between 30 °C and 35 °C.

3. Results and Discussion

3.1. Paper-LIG from activated charcoal filter paper

Commonly, the formation of laser-induced graphene from paper requires two irradiation steps. The first one converts the cellulose of the paper into aromatic char. To this end, the paper usually must be treated beforehand with a fire-retardant compound, in order to prevent the volatilization of the cellulose.[13] We note that irradiation under inert atmosphere is a viable alternative to the use of fire-retardants, as has been reported for the synthesis of LIG from wood.[12] However, this requires a more complicated setup. Moreover, one must consider the active role of the phosphate-based fire retardant in the synthesis process, as the phosphate groups promote the dehydration of cellulose, preventing its decomposition into levoglucosan and further volatilization, as has also been reported previously.[16] Then, the second laser irradiation step leads to the graphitization of the aromatic char into a graphene-based material. As such, it becomes appealing to explore the formation of laser-induced graphene from papers already containing amorphous carbon components, with filter paper containing activated charcoal presenting itself as an example of such precursors.

In a typical laser-induced graphene synthesis experiment, the laser beam is scanned over the precursor paper along straight lines filling up the area to be irradiated. Here, the varied parameters were irradiation power, scan speed and separation between the scan lines (the position of the sample relative to the laser head was fixed at 9 mm below

focus for the first step, while the second one was performed in focus). Figure 1 shows secondary electron scanning electron microscopy (SE-SEM) images of the samples obtained at different irradiation powers and scan speeds, at 100 µm line separation. For lower irradiation power one can see that the fibers retain more of their original shape and structure than for higher power. The porosity appears to increase with the irradiation power, with more voids in the fibers irradiated at higher power. Lower scan speed also seems to lead to greater porosity inside the fibers, which can be explained by the fact that a lower scan speed implies that the laser beam remains for a longer period of time at each point along the scanned lines, delivering more energy at each such point. This is consistent with what has been reported for common filter paper,[14] with greater porosity signaling a more extensive transformation of the cellulose fibers into laser-induced graphene. However, it can also be seen that as the porosity development becomes more extensive there is greater damage to the fibers, as each fiber loses its structural integrity. This is reflected in the sheet resistance measurements of the obtained samples (Figure 2(a)). Here, one can see a trend where, for irradiation power of 700 mW and 800 mW, lower scan speed results in more conductive samples, up to the point where the scan speed becomes too low and the energy delivered at each point along the scanned region becomes too large, leading to the damage of the top layers of the transformed paper. Interestingly, however, for an even further irradiation power increase this tendency is inverted for scan speeds lower than 40 mm s^{-1}, with the sheet resistance being lower for slower scan speed. This can be explained by the irradiation power being high enough to allow a fast removal of the top layers of the laser-induced graphene with enough time remaining for the graphitization of the remaining ones (but not enough for them to suffer extensive damage and be removed as well). Additionally, Figure 2(a) shows that, in general, smaller line separations result in less conductive samples, potentially due to the increase damage suffered by the irradiated material with on account of the larger overlap between the scan lines. Finally, in what concerns the crystalline quality of the obtained material, Raman spectroscopy of the most conductive samples presents the characteristic spectra of laser-induced graphene, characterized by a sharp and narrow G peak and a symmetrical 2D peak, with the respective intensity ratio, I_{2D}/I_G, of ~0.5 (Figure 2(b), bottom). As for the D peak, while it indicates the presence of disorder, it is common in LIG.[8] We also note that the less conductive samples predominantly show spectra representative of amorphous carbon (Figure 2(b), top), indicating that the reason behind their high sheet resistances is incomplete

graphitization. In the case of samples formed at 800 mW and low scan speed, this provides further support to the idea that there is a removal of the upper layers of the irradiated paper, revealing poorly transformed material underneath.

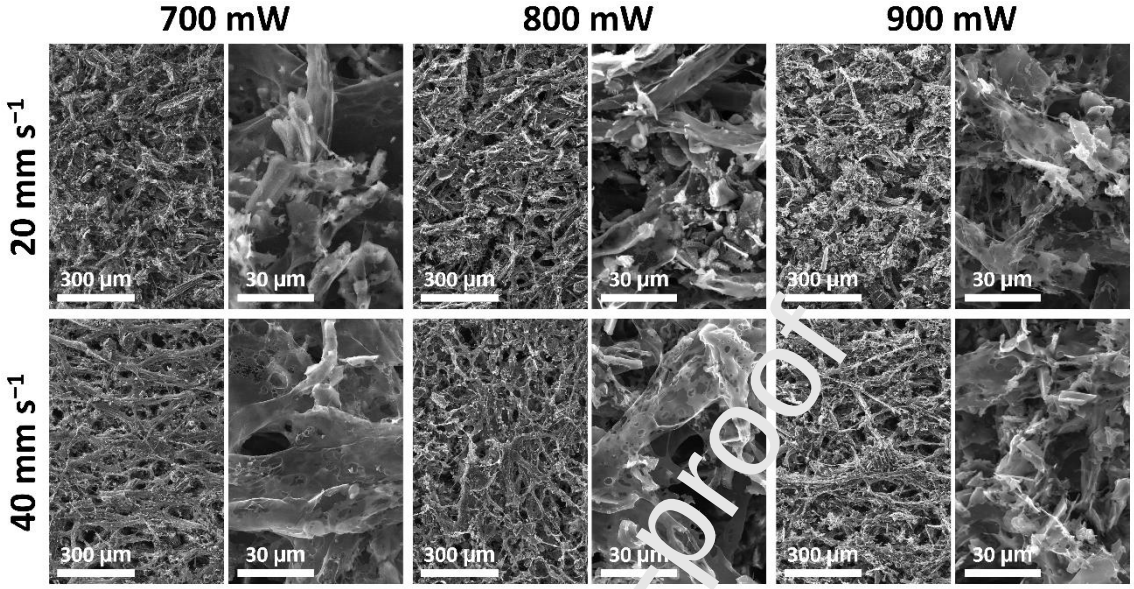

Figure 1. SE-SEM images of laser-induced graphene formed on activated charcoal filter paper, for different irradiation powers and scan speeds, at 0.1 mm scan line separation.

Overall, it appears that the presence of activated charcoal does not provide substantial advantage to the process of formation of laser-induced graphene from paper. However, one has to consider the role of the other additives present in this type of paper, with energy dispersive X-ray spectra (EDS) of the paper revealing the presence of elements such as Mg, Si, Ca and Fe. These can be attributed to inorganic fillers, which are additives commonly used in the papermaking process.[24] Thus, we argue that these additives cover the underlying fibers from the incident laser radiation, which leads to incomplete graphitization in these region and, consequently, low conductivity, with even the most conductive samples presenting sheet resistances nearly five times larger than those obtained with hardened ashless filter paper without any additives.[14] Still, the high quality of the synthesized material, as indicated by the Raman spectra of the most conductive samples, show that activated charcoal filter paper can function as a

LIG precursor.

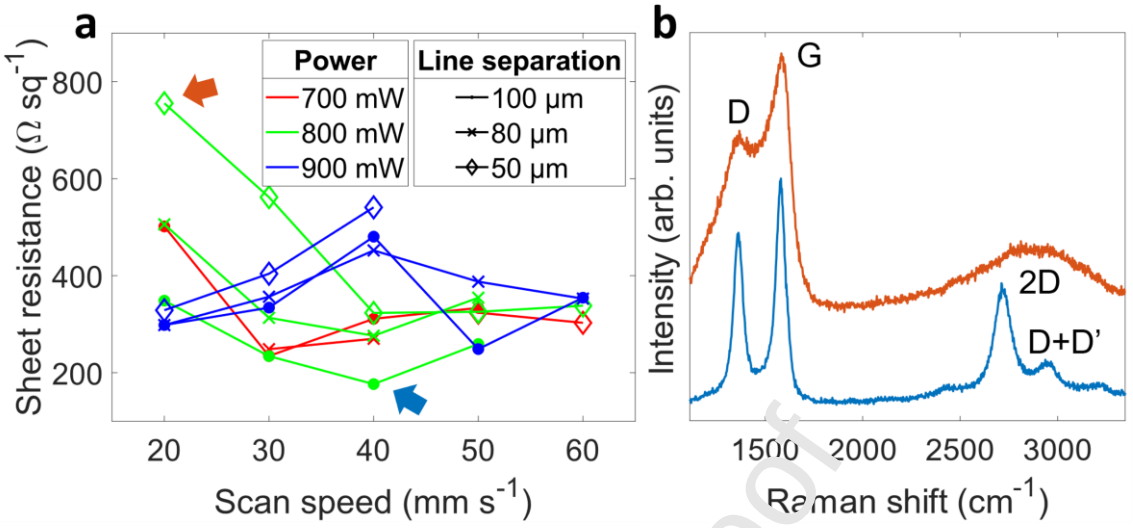

Figure 2. (a) Sheet resistance of *paper-LIG* samples synthesized on activated charcoal filter paper at different irradiation powers, scan line separations and scan speeds. **(b)** Raman spectra of the most (top) and least (bottom) resistive samples (identified in (a) by colored arrows).

3.2. Paper-LIG with a single irradiation

The formation of laser-induced graphene on materials such as paper is a two-step process, where the first irradiation, performed with the sample out of focus, converts the cellulose into char, and the second one, done in focus, graphitizes this char into laser-induced graphene. However, any future commercial application of this material could benefit if it were possible to obtain it using just a single irradiation step. This would halve the synthesis time, which would represent a significant productivity gain, particularly for scaled up production.

Figure 3(a) shows a photograph of a sample obtained by scanning the laser beam once over fire-retardant treated filter paper. Extensive damage of the paper can be seen, with the yellow backlight revealing perforations along the lines scanned by the laser. However, as the separation between the scan lines is reduced, this damage becomes less extensive, with fewer perforations visible (Figure 3(b-d)). The sample obtained with a line separation of 30 µm is fairly continuous, with only a few through holes visible, while SE-SEM cross-section images reveal an ~85 µm layer of transformed fibers (Figure 3(e)). Moreover, the sample shows a blacker coloration indicative of a more

complete transformation of the irradiated cellulose, which is confirmed by Raman spectroscopy, indicating that LIG was obtained (Figure 3(f)).

These observations can be explained as follows. When the laser beam is scanned over the paper, due to the gaussian intensity profile of the beam, the central part of the scanned line is ablated due to the high peak fluence of the focused laser (Figure 3(g)). However, in the periphery of the scanned line, where the fluence is lower, the irradiated paper gets charred without ablation. This charred material is more resistant to laser damage, so when the next adjacent line is scanned by the beam, if the lines are sufficiently close to ensure the overlapping of the irradiated regions, the beam will pass over the char formed by the previous scan, and it will get graphitized into laser-induced graphene without getting ablated (as seen in Figure 3(e)). If, however, the line separation is too large, each new one will pass over non-charred paper, which will get ablated due to its lower resistance to damage, resulting in perforations seen in Figure 3(a-c). This also explains the presence of an extensive cut at the top of the sample in Figure 3(d), as the first line necessarily passes over non-charred paper, resulting in ablation along this line. In our experimental setup the laser beam diameter at focus was determined to be 140 μm, so to ensure that each subsequent scanning line passes inside the area irradiated by the previous one, the line separation must be below 70 μm. This is why already at 50 μm one begins to see some black colored material reminiscent of LIG. Still, one has to take into account that the charring at the edges of the affected area is not as extensive as near the center of the scanned line, so a further decrease in line separation, down to 30 μm, is necessary for the subsequent lines to pass over sufficiently charred cellulose, as confirmed by Figure 3(d).

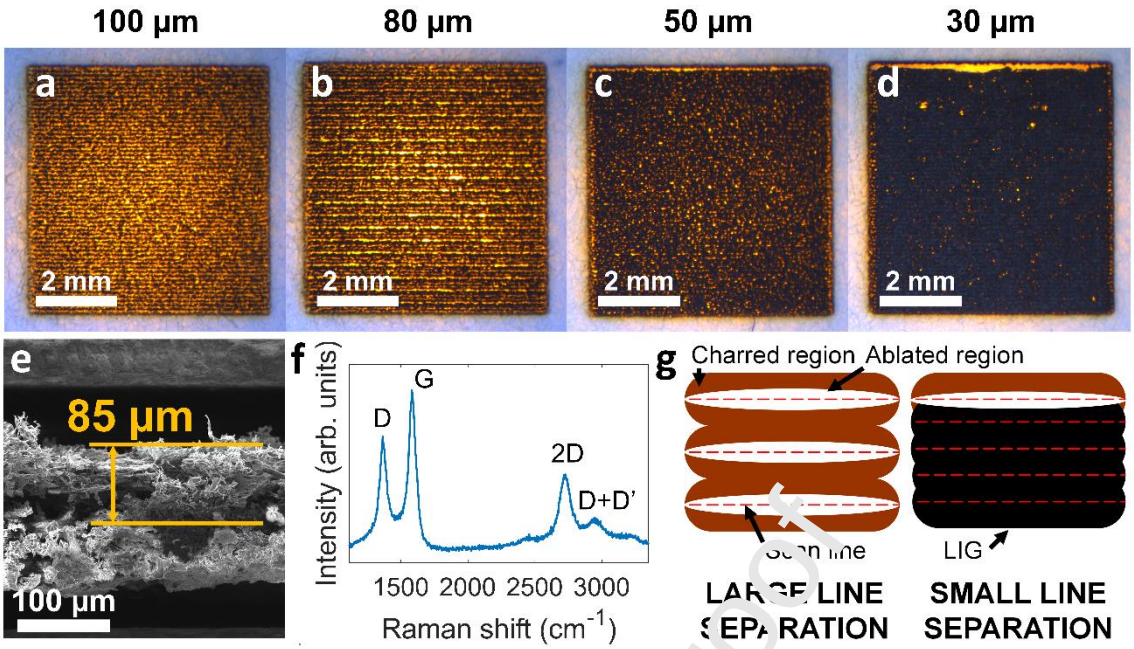

Figure 3. (a-d) Photographs of samples obtained after single scan irradiation (in focus) of filter paper, at scan line separations of 100 µm, 80 µm, 50 µm and 30 µm, respectively. **(e)** SE-SEM cross-section image and **(f)** representative Raman spectrum of the *paper-LIG* sample in (d). **(g)** Illustration of how a reduced scan line separation allows to obtain LIG with a single scan. Each time the laser beam passes over the regions charred when scanning the previous line, these regions convert into LIG without ablation.

The general observation that smaller line separations result in less perforated samples is confirmed by SE-SEM images of samples obtained with different irradiation powers and distance between lines (Figure 4). Separations of 80 µm and 50 µm lead to ablation along the scanned lines, which gets more pronounced at higher irradiation powers. With a line separation of 30 µm, however, even at 900 mW the sample shows no through holes. Moreover, with large line separations the remaining material appears to be poorly transformed, showing limited porosity development and thicker fiber walls. On the contrary, a line separation of 30 µm yields a thin, porous, veil-like material characteristic of *paper-LIG*, even at irradiation powers as low as 700 mW. This feature is in accordance with the above proposed explanation, as with larger line separations the charred paper does not undergo a second irradiation by the subsequent scan of the laser beam passing over the next line.

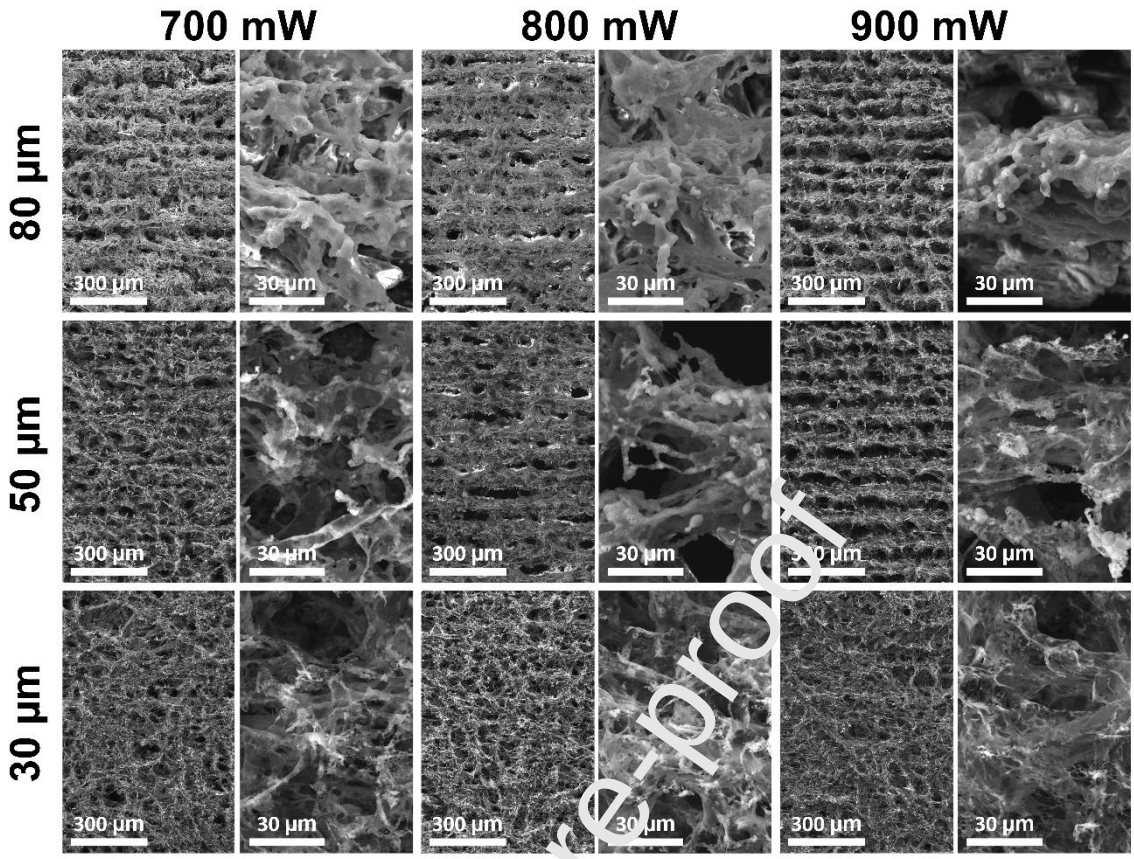

Figure 4. SE-SEM images of laser-induced graphene formed on filter paper, for different irradiation powers and scan line separation, at a scan speed of 40 mm s^{-1}.

Figure 5(a) shows photographs of samples obtained using different irradiation powers and scan speeds. While increasing the irradiation power results in fewer through holes, in agreement with the discussion above, a combination of high power and low scan speed can lead to the crumbling of the resulting material. This is similar to what was observed for activated charcoal filter paper, where excessive energy delivery originates the loss of the structural integrity of the fiber, and has also been reported for *paper-LIG* formed using two irradiation steps.[14]

The sheet resistance measurements, presented in Figure 5(b), reflect the ideas discussed in this section. In general, smaller line separation and higher irradiation energy gives more conductive samples. Moreover, there is a trend where lower scan speeds result in smaller sheet resistances, up to the point where the energy delivered to the irradiated substrate becomes too large and the samples lose their structural integrity by cracking

and crumbling. In these cases, even though the obtained material might be highly conductive, no sheet resistance values can be obtained.

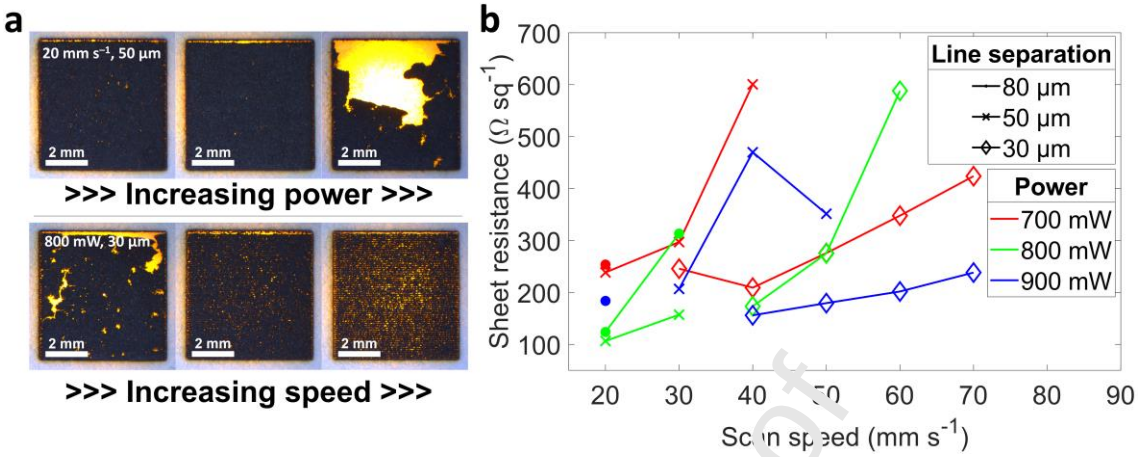

Figure 5. (a) Photographs of samples obtained after single scan irradiation (in focus) of filter paper, at irradiation powers of 700 mW, 800 mW and 900 mW (top) and scan speeds of 30 mm s^{-1}, 40 mm s^{-1} and 50 mm s^{-1} (bottom). **(b)** Sheet resistance of *paper-LIG* samples synthesized with single scan irradiation (in focus) filter paper, at different irradiation powers, scan line separations and scan speeds.

On balance, *paper-LIG* can be obtained after a single irradiation step in focus, as long as the separation between the scan lines is small enough to ensure overlap. In this case, the two irradiation steps are essentially replicated by the repeated irradiation of the same regions by adjacent scan lines. Higher irradiation energies and lower scan speeds lead to more conductive samples, up to a limit where the samples begin to crack and crumble due to the loss of the structural integrity of the fibers as they become thinner and more porous. Compared to the conventional approach involving two irradiation steps, the *paper-LIG* obtained here presents a slightly more fragile appearance with a bit more damage to the fibers.[14] This is also reflected in a somewhat larger sheet resistance than the one reported for double-irradiated *paper-LIG*. However, the obtained material is still very conductive, while benefitting from a faster synthesis process. This is particularly important when exploring the low-cost and environmentally friendly applications enabled by *paper-LIG*, with the efficiency of the synthesis process being as important as the material itself.

3.3. Paper-LIG from xylan and its application in temperature sensing

Beside cellulose, there are other abundant structural biopolymers present in plants which are often underutilized. With vast amounts of biomass residues/subproducts generated by agriculture every year, there is a growing interest in its valorization. The most abundant components of plant-based biomass, beside cellulose, are lignin and hemicellulose, with xylan being the most common type of the latter in vascular plants.[25] Throughout the last several decades xylan has been proposed for several application fields, with potential in wound dressings, coatings or as a pharmaceutical auxiliary, for example.[26] As such, it becomes appealing to explore xylan as a precursor for LIG synthesis, which we undertake by irradiating carboxymethyl xylan films prepared by the solvent casting method. Two irradiation steps were employed, with the film being fixed at 9 mm below focus during the first one and in focus during the second one. The laser power was set to ~1 W, the scan speed was 30 mm s^{-1} and the line separation was 0.1 mm. Figure 6(a) shows a photograph of the material obtained after irradiation. While some through holes can be observed, overall it presents the dark color characteristic of laser-induced graphene. Raman spectroscopy allows to confirm it as LIG (Figure 6(b)). The observed transformation of carboxymethyl xylan into laser-induced graphene is further illustrated by the porosity development seen in SE-SEM images, although some heterogeneity can be seen (Figure 6(c)). This porosity is typical of laser-induced graphene obtained from both commercial polymers[8] and cellulose paper.[14] Compared to the latter, however, xylan-derived LIG presents a denser structure. The lack of long, porous fibers such as the ones seen in *paper-LIG* can be explained by the less fibrous morphology of the carboxymethyl xylan precursor. Additionally, the thickness of the LIG layer was measured at ~80 µm (Figure 6(d)). This is slightly thinner that what has been observed for *paper-LIG* (~100 µm),[14] potentially due to the denser nature of the xylan film, which should result in a shallower penetration depth of the laser beam during synthesis. The sheet resistance of the LIG obtained from carboxymethyl xylan was measured at 186 Ω sq^{-1}.

These results provide a solid basis for the application of laser-induced graphene obtained from xylan in devices such as sensors. To better demonstrate this, we develop a simple, low-cost and environmentally friendly temperature sensor employing this material. To this end, a 6×12 mm^2 conductive path was obtained by laser irradiation of the modified xylan film (an output power of ~1.5 W was used). Then, the resistance along this path was measured in response to different temperatures (controlled by a

Peltier element), in the range of 20 °C to 45 °C. Figure 6(e) shows real-time monitoring of the sensor's response to two sweeps where the temperature was varied several times between 20 °C and 45 °C in steps of 5 °C. Additionally, the temperature was repeatedly set at either 30 °C or 35 °C to evaluate the reproducibility and stability of the measured resistances at each temperature. Lastly, sweeps between 30 °C and 35 °C in 1 °C steps were performed. A magnified view of these can be seen in Figure 6(f), demonstrating the sensor's ability to reproducibly resolve temperature changes of 1 °C. Overall, the response is stable and reproducible, and the resistance values stabilize quickly at each temperature.

Interestingly, the resistance decreases with temperature. The negative temperature coefficient is consistent with the trend previously reported for both laser-induced graphene from polyimide[27,28] and for reduced graphene oxide (rGO).[29,30] In the case of the latter, it has been ascribed to the increase of the number of charge carriers with temperature, as well as to hopping and tunneling between adjacent rGO sheets, with the increase in temperature allowing to overcome potential barriers. A similar explanation has been recently given for the temperature response of glass-like carbon obtained by laser irradiation of polyimide.[31] Likewise, recently the concept of temperature dependent hopping (more specifically variable range hopping) has been employed to describe the electronic conduction mechanism (and, correspondingly, its temperature dependence) in *paper-LIG* formed under UV laser.[32]

In Figure 6(g), the resistance values measured during the four sweeps in the range between 45 °C and 20 °C in steps of 5 °C were used to determine the calibration curve of the sensor (the values corresponding to the last 30 s at each temperature were used). The response is confirmed to be linear (coefficient of determination, r^2, of 0.998) and the sensitivity has a value of $-1.29\ \Omega\ °C^{-1}$, demonstrating the potential of this material for sensing applications. For example, taking into consideration the prospective application of xylan as an effective barrier coating for packaging papers,[33] this could open new opportunities for sensing solutions in food packing materials.

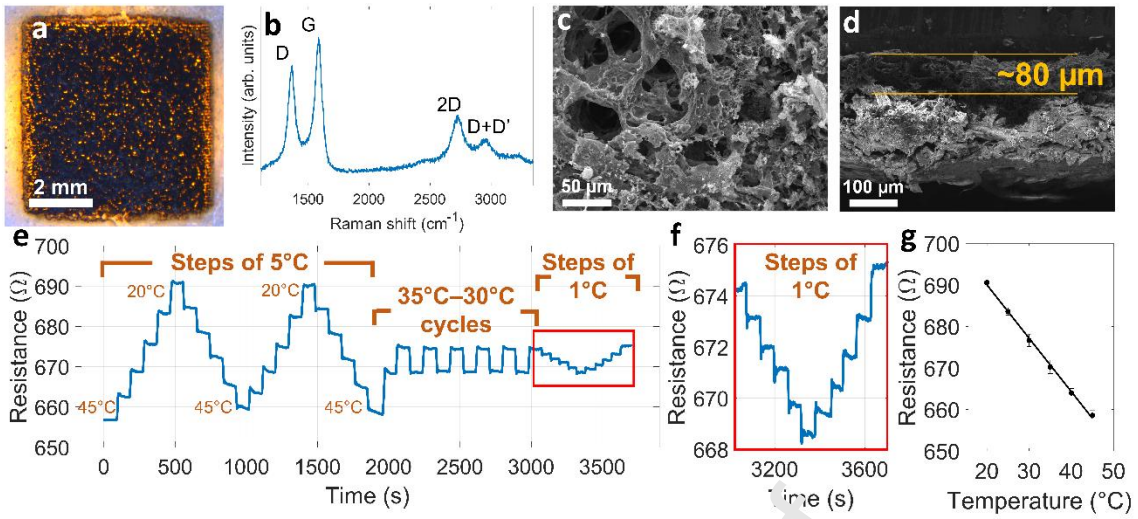

Figure 6. (a) Photograph of the sample obtained by laser irradiation of the carboxymethyl xylan film. **(b)** Raman spectrum of the sample in (a), showing the characteristic signature of laser-induced graphene. **(c)** SE-SEM image of LIG obtained from modified xylan. **(d)** Cross-section SE-SEM image of LIG obtained from xylan, showing the thickness of the LIG. **(e)** Real-time measurements of the resistance along the conductive path formed by laser irradiation of the carboxymethyl xylan film in response to different temperatures. Showcased are sweeps where the temperature was varied several times between 20 °C and 45 °C in steps of 5 °C, repeating cycles between 30 °C and 35 °C, as well as sweeps between 30 °C and 35 °C in 1 °C steps. **(f)** Amplified view of the sweeps between 30 °C and 35 °C (highlighted in (e) by a red frame), showing the sensor's ability to reproducibly resolve temperature changes of 1 °C. **(g)** Calibration curve of the temperature sensor employing LIG obtained from modified xylan, showing good linearity (r^2=0.998).

4. Conclusions

In this work, we presented a systematic study of the formation of *paper-LIG*, a versatile porous 3D graphene material obtained by laser irradiation of paper, on activated charcoal filter paper. Moreover, we reported the synthesis of *paper-LIG* with a single irradiation step, improving upon the conventional multiple lasing approach. These results are accompanied by a description of the conditions and mechanisms that allow this simplified synthesis, where the scan line separation must be reduced to ensure the overlap of adjacent beam paths. Lastly, we show that laser-induced graphene can be

obtained by irradiation of fire-retardant treated xylan film, which is an abundant, environmentally friendly biopolymer. The obtained material is then employed as a proof-of-concept temperature sensor, showing a sensitivity of –1.29 Ω °C^{-1}. Overall, this work contributes to a better understanding of the laser-induced graphene synthesis process, complementing the array of precursor substrates and resulting materials in this field. This encourages future applications in flexible, conductive, and environmentally friendly devices.

CRediT authorship contribution statement

Bohdan Kulyk: Conceptualization, Investigation, Software, Methodology, Writing - original draft, Writing - review & editing. **Marina Matos:** Conceptualization, Investigation, Methodology, Writing - review & editing. **Beatriz Silva:** Conceptualization, Investigation, Methodology, Writing - review & editing. **Alexandre Carvalho:** Conceptualization, Investigation, Methodology, Software, Writing - review & editing. **António Fernandes:** Conceptualization, Investigation, Methodology, Writing - review & editing. **Dmitry Evtuguin:** Conceptualization, Methodology, Supervision, Writing - review & editing. **Elvira Fortunato:** Writing - review & editing. **Florinda Costa:** Conceptualization, Methodology, Supervision, Writing - review & editing.

Declaration of competing interest

The authors declare that they have no known competing financial interests or personal relationships that could have appeared to influence the work reported in this paper.

Acknowledgements

This work was developed within the scope of the project i3N (UIDB/50025/2020, and UIDP/50025/2020), financed by national funds through the Portuguese Foundation for Science and Technology/MCTES (FCT I.P.). This work was also financially supported by the CICECO – Aveiro Institute of Materials, within the scope of the projects UIDB/50011/2020 and UIDP/50011/2020, financed by national funds through the FCT I.P. B. Kulyk acknowledges the Ph.D. grant SFRH/BD/141525/2018 by FCT I.P. E. Fortunato acknowledges the European Research Council AdG grant 787410 from the project DIGISMART.

References

[1] Novoselov K S, Geim A K, Morozov S V., Jiang D, Zhang Y, Dubonos S V., Grigorieva I V. and Firsov A A 2004 Electric field effect in atomically thin carbon films *Science* **306** 666–9

[2] Ferrari A C, Bonaccorso F, Fal'ko V I, Novoselov K S, Roche S, Bøggild P, Borini S, Koppens F H L, Palermo V, Pugno N M, Garrido J A, Sordan R, Bianco A, Ballerini L, Prato M, Lidorikis E, Kivioja J, Marinelli C, Ryhänen T, Morpurgo A F, Coleman J N, Nicolosi V, Colombo L, Fert A, Garcia-Hernandez M, Bachtold A, Schneider G F, Guinea F, Dekker C, Barbone M, Sun Z Z, Galiotis C, Grigorenko A N, Konstantatos G, Kis A, Katsnelson M I, Vandersypen L M K, Loiseau A, Morandi V, Neumaier D, Treossi E, Pellegrini V, Polini M, Tredicucci A, Williams G M, Hee Hong B, Ahn J-H, Min Kim J, Zirath H, van Wees B J, van der Zant H, Occhipinti L, Di Matteo A, Kinloch I A, Seyller T, Quesnel E, Feng X L, Teo K B K, Rupesinghe N L, Hakonen P J, Neil S R T, Tannock Q, Löfwander T and Kinaret J M 2015 Science and technology roadmap for graphene, related two-dimensional crystals, and hybrid systems *Nanoscale* **7** 4598–810

[3] Banszerus L, Schmitz M, Engels S, Goldsche M, Watanabe K, Taniguchi T, Beschoten B and Stampfer C 2016 Ballistic Transport Exceeding 28 μm in CVD Grown Graphene *Nano Lett.* **16** 1387–91

[4] Kulyk B, Carvalho A F, Fernandes A J S and Costa F M 2020 Millimeter sized graphene domains through in situ oxidation/reduction treatment of the copper substrate *Carbon* **169** 403–15

[5] Li Z, Young R J, Backes C, Zhao W, Zhang X, Zhukov A A, Tillotson E, Conlan A P, Ding F, Haigh S J, Novoselov K S and Coleman J N 2020 Mechanisms of Liquid-Phase Exfoliation for the Production of Graphene *ACS Nano* **14** 10976–85

[6] Kulyk B, Freitas M A, Santos N F, Mohseni F, Carvalho A F, Yasakau K, Fernandes A J S, Bernardes A, Figueiredo B, Silva R, Tedim J and Costa F M 2021 A critical review on the production and application of graphene and graphene-based materials in anti-corrosion coatings *Crit. Rev. Solid State Mater.*

Sci. **0** 1–48

[7] Ye R, James D K and Tour J M 2019 Laser-Induced Graphene: From Discovery to Translation *Adv. Mater.* **31** 1–15

[8] Lin J, Peng Z, Liu Y, Ruiz-Zepeda F, Ye R, Samuel E L G G, Yacaman M J, Yakobson B I and Tour J M 2014 Laser-induced porous graphene films from commercial polymers *Nat. Commun.* **5** 1–8

[9] Carvalho A F, Fernandes A J S, Leitão C, Deuermeier J, Marques A C, Martins R, Fortunato E and Costa F M 2018 Laser-Induced Graphene Strain Sensors Produced by Ultraviolet Irradiation of Polyimide *Adv. Funct. Mater.* **28** 1–8

[10] Carvalho A F, Fernandes A J S, Martins R, Fortunato E and Costa F M 2020 Laser- Induced Graphene Piezoresistive Sensors Synthesized Directly on Cork Insoles for Gait Analysis *Adv. Mater. Technol.* 2000630

[11] Carvalho A F, Kulyk B, Fernandes A J S, Fortunato E and Costa F M 2021 A Review on the Applications of Graphene in Mechanical Transduction *Adv. Mater.* 2101326

[12] Ye R, Chyan Y, Zhang J, Li Y, Han X, Kittrell C and Tour J M 2017 Laser-Induced Graphene Formation on Wood *Adv. Mater.* **29** 1–7

[13] Chyan Y, Ye R, Li Y, Singh S P, Arnusch C J and Tour J M 2018 Laser-Induced Graphene by Multiple Lasing: Toward Electronics on Cloth, Paper, and Food *ACS Nano* **12** 2176–83

[14] Kulyk B, Silva B F R, Carvalho A F, Silvestre S, Fernandes A J S, Martins R, Fortunato E and Costa F M 2021 Laser-Induced Graphene from Paper for Mechanical Sensing *ACS Appl. Mater. Interfaces* **13** 10210–21

[15] Zang X, Shen C, Chu Y, Li B, Wei M, Zhong J, Sanghadasa M and Lin L 2018 Laser-Induced Molybdenum Carbide-Graphene Composites for 3D Foldable Paper Electronics *Adv. Mater.* **30** 1800062

[16] Yao Y, Duan X, Niu M, Luo J, Wang R and Liu T 2019 One-step process for direct laser writing carbonization of NH4H2PO4 treated cellulose paper and its use for facile fabrication of multifunctional force sensors with corrugated structures *Cellulose* **26** 7423–35

[17] Lee S and Jeon S 2019 Laser-Induced Graphitization of Cellulose Nanofiber Substrates under Ambient Conditions *ACS Sustain. Chem. Eng.* **7** 2270–5

[18] de Araujo W R, Frasson C M R, Ameku W A, Silva J R, Angnes L and Paixão T R L C 2017 Single-Step Reagentless Laser Scribing Fabrication of Electrochemical Paper-Based Analytical Devices *Angew. Chemie - Int. Ed.* **56** 15113–7

[19] Lee S, Jang H, Lee H, Yoon D and Jeon S 2019 Direct Fabrication of a Moisture-Driven Power Generator by Laser-Induced Graphitization with a Gradual Defocusing Method *ACS Appl. Mater. Interfaces* **11** 26970–5

[20] Chyan Y, Cohen J, Wang W, Zhang C and Tour J M 2019 Graphene Art *ACS Appl. Nano Mater.* **2** 3007–11

[21] Zhao P, Bhattacharya G, Fishlock S J, Guy J G M, Kumar A, Tsonos C, Yu Z, Raj S, McLaughlin J A, Luo J and Soin N 2020 Replacing the metal electrodes in triboelectric nanogenerators: High-performance laser-induced graphene electrodes *Nano Energy* **75** 104956

[22] Gomes T M P, Mendes De Sousa A P, Belenkiy Y I and Evtuguin D V. 2020 Xylan accessibility of bleached eucalypt pulp in alkaline solutions *Holzforschung* **74** 141–8

[23] Petzold K, Schwikal K, Günther W and Heinze T 2005 Carboxymethyl Xylan - Control of Properties by Synthesis *Macromol. Symp.* **232** 27–36

[24] Velho J L 2003 *Mineral fillers for paper: why, what, how* (TECNICELPA Technical books)

[25] Ebringerová A 2005 Structural Diversity and Application Potential of Hemicelluloses *Macromol. Symp.* **232** 1–12

[26] Deutschmann R and Dekker R F H 2012 From plant biomass to bio-based chemicals: Latest developments in xylan research *Biotechnol. Adv.* **30** 1627–40

[27] Stanford M G, Yang K, Chyan Y, Kittrell C and Tour J M 2019 Laser-Induced Graphene for Flexible and Embeddable Gas Sensors *ACS Nano* **13** 3474–82

[28] Bobinger M R, Romero F J, Salinas-Castillo A, Becherer M, Lugli P, Morales D

P, Rodríguez N and Rivadeneyra A 2019 Flexible and robust laser-induced graphene heaters photothermally scribed on bare polyimide substrates *Carbon* **144** 116–26

[29] Han R, Wang L, Tang X, Qian J, Yu J, Chen X and Huang Y 2021 Facile fabrication of rGO/LIG-based temperature sensor with high sensitivity *Mater. Lett.* **304** 130637

[30] Dan L and Elias A L 2020 Flexible and Stretchable Temperature Sensors Fabricated Using Solution- Processable Conductive Polymer Composites *Adv. Healthc. Mater.* **9** 2000380

[31] Gandla S, Naqi M, Lee M, Lee J J, Won Y, Pujar P, Kim J, Lee S and Kim S 2020 Highly Linear and Stable Flexible Temperature Sensors Based on Laser-Induced Carbonization of Polyimide Substrates for Personal Mobile Monitoring *Adv. Mater. Technol.* **5** 2000014

[32] Kulyk B, Silva B F R, Carvalho A F, Barbosa P, Girão A V., Deuermeier J, Fernandes A J S, Figueiredo F M L, Fortunato E and Costa F M 2021 Laser-Induced Graphene from Paper by Ultraviolet Irradiation: Humidity and Temperature Sensors *Adv. Mater. Technol.*

[33] Ramos A, Sousa S, Evtuguin D V. and Gamelas J A F 2017 Functionalized xylans in the production of xylan-coated paper laminates *React. Funct. Polym.* **117** 89–96

Graphical abstract

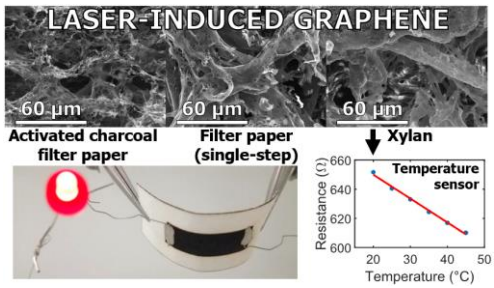

Highlights

- Synthesis of laser-induced graphene from filter paper by a single irradiation step.
- Synthesis of laser-induced graphene by irradiation of filter paper containing activated charcoal.
- Laser-induced graphene from a xylan substrate, valorizing this underutilized natural product.
- Temperature sensor employing laser-induced graphene obtained from modified xylan.